Applied Energy 278 (2020) 115699

Contents lists available at ScienceDirect

Applied Energy

journal homepage: www.elsevier.com/locate/apenergy

Estimation of parameters affected in internal exhaust residual gases recirculation and the influence of exhaust residual gas on performance and emission of a spark ignition engine

Nguyen Xuan Khoa [a,b], Y. Quach Nhu [a], Ocktaeck Lim [a,*]

[a] Graduate School of Mechanical Engineering, University of Ulsan, 93 Daehak-ro, Nam-gu, Ulsan 44610, South Korea
[b] Faculty of Automobile Technology of HaNoi University of Industry, No.298, Cau Dien Street, Bac Tu Liem District, Ha Noi, Viet Nam

ARTICLE INFO

Keywords:
Residual gas
Effective release energy
Peak firing pressure rise
Peak firing temperature
Emission characteristics

ABSTRACT

In the effort of improving the internal combustion engine performance, the exhaust residual gases and effective release energy are sensitive factors, which effect on engine efficiency and emission formation. Herewith we estimated and summarized the parameters which affect the internal exhaust residual gases recirculation, and investigate the effect of internal exhaust residual gas on peak pressure rise, effective energy, and engine emissions, which weren't presented yet in the previous articles. It is knotty to investigate the residual gas ratio, the effective energy under the various testing conditions from the experiments. Through the simulation and experiment methods approach we eliminated certain above drawbacks. From results of the research, we thoroughly investigated the effects of engine speed, air–fuel ratio, valve overlap, combustion duration, intake port diameter-bore ratio, and bore-stroke ratio on the internal exhaust residual gases recirculation. We also found that the increase in the internal exhaust residual gas from 1% to 5% was due to the peak firing temperature decrease from 2900 K to 1250 K, the peak pressure rise decrease from 8 to 5.5 bar/deg, the effective release energy decrease from 0.85 to 0.53 kJ, the NO_x emission reduction from 11.3 to 2.12 g/kwh and the engine brake torque decrease from 20.3 to 9 Nm.

1. Introduction

In spark ignition engines, the exhaust residual gases and effective release energy are known as sensitive factors, which effect on engine performance. Some internal exhaust residual gases are returned the cylinder through the exhaust valve port. This residual gas will premix with the intake fresh air–fuel mixture and affect combustion stability, charge mass, flame speed, and emission of toxic products. The exhaust gas recirculation (EGR) is an effective method to reduce the NO_x emissions [1–3], decrease the PM emission [4,5] of the compression ignition engine. In the spark ignition engine, the exhaust gas recirculation was applied to improve engine thermal efficiency and reduce NO_x emission [6,7].

From the historical trend of the factors which affect the mass of exhaust residual gas in the cylinder, the effects of internal residual gas recirculation on engine performance, and emission formation. Past researchers attempting to control the amount of residual gas trapped in the cylinder and used new techniques to measure exhaust residual gas, such as Variable Valve Timing technologies [8,9], changing exhaust valve closing timing [10], and an exhaust gas prediction method [11,12]. Because it is knotty to investigate the internal residual gas recirculation and the effective release energy through doing experiments with various testing conditions, the computational analysis method is useful and effective solution to solve this problem.

Thompson Diórdinis Metzka Lanzanova et al. [13] built a one-dimensional model in GT-Power to investigate the influence of valve timing strategies on the exhaust residual gas factors of a Ricardo Hydra camless spark ignition (SI) engine fueled with wet ethanol. The engine was operated at a partial load condition and 1500 rpm of engine speed. They discovered that an increased percentage of water in the wet ethanol led to an increase in the residual gas fraction, which in turn led to an increase in the maximum pressure in the cylinder.

Stanislaw Szwaja et al. [14] performed an experiment on a single-cylinder Hydra engine with natural gas fuel using a variable valve overlap to study the effect of exhaust residual gas on engine emission

* Corresponding author.
E-mail address: otlim@ulsan.ac.kr (O. Lim).

https://doi.org/10.1016/j.apenergy.2020.115699
Received 5 November 2019; Received in revised form 22 June 2020; Accepted 13 August 2020

Nomenclature

BDC	Bottom dead centre
TDC	Top dead centre
BTDC	Before top dead centre
ATDC	After top dead centre
BSFC	Brake specific fuel consumption, (g/KWh)
BMEP	Brake mean effective pressure, (Bar)
IMEP	Indicated mean effective pressure, (Bar)
FMEP	Friction mean effective pressure, (Bar)
SMEP	Scavenging mean effective pressure, (Bar)
HC	Hydrocarbon
PM	Particulate matter
THC	Total hydrocarbon emissions
CA	Crank angle, deg
ERG	Exhaust gas recirculation
SI-engine	Spark ignition engine
CI-engine	Combustion ignition engine
IPD/B	Intake port diameter-Bore ratio, (–)
A/F	Air per fuel ratio, (–)
Q	Total fuel heat input, (W)
α	Crank angle, (deg)
α_0	Start of combustion, (deg)
$\Delta\alpha_c$	Combustion duration, (deg)
m	Shape parameter, (-)
a	Vibe parameter
Q_T	Heat lost to the wall, (W/m^2)
A	Total surface area of cylinder head, piston and cylinder, (m^2)
q_{coeff}	Heat transfer coefficient, (W/m^2 K)
T_c	Combustion gas temperature, (K)
T_w	Wall temperature of cylinder (K)
$\frac{dm}{dt}$	Air mass flow rate (–)
A_{eff}	Effective flow area (–)
P_1	Upstream stagnation pressure, (Pa)
T_1	Upstream stagnation temperature, (K)
P_2	Downstream static pressure, (Pa)
K	Ratio of specific heats (–)
x_{SOC}^{cp}	Residual gas at start of combustion (SOC)
ρ	Local cylinder density (kg/m^3)
x^{cp}	Local cylinder combustion product mass fraction at SOC
V_D	Displacement volume, (m^3)
r_i	Demotes reaction rates of table 2 and 3 (mole/cm^{3}s)
C_p	Denotes post processing multiplier, (–)
C_K	Denotes kinetic multiplier, (–)
m_{HC}	Mass of unburned charge in the crevices (kg)
P_c	Cylinder pressure (Pa)
$V_{crevice}$	Total crevice volume (m^3)
M	Unburned molecular weight (kg/kmol)
R	Gas constant (J/(kmol·K))
T_{piston}	Piston temperature (K)
m_{air}	Air mass flow [kg/s]
AFR	Air-fuel ratio (–)
n	Engine speed (rpm)
T_{eff}	Engine effective torque, (Nm)
K_{cycle}	Simulation cycle parameter, (cycle)

characteristics. The tests were performed at engine speeds of 1250 rpm and 2000 rpm. They found that the residual gas in the cylinder had the most effect on the combustion stability and engine toxic emissions. An increase of exhaust residual gas led to a decrease in NO_x and an increase in both HC and CO. In this case a 28% increase of residual gas led to a 67% decrease in NO_x, the main combustion phase was improved by 20%, and the flame rate increased by 28%.

Roberto Berlini Rodrigues da Costa et al. [15] presented a study on the influence of EGR on engine combustion and engine emissions of a natural gas-hydrous ethanol dual-fuel SI engine. In that experimental setup a single-cylinder AVL 5495 SCRE engine was conducted. The testing engine speed was 1800 rpm and the stoichiometric air–fuel condition was maintained at 4 bars. A 1-D combustion model was created in the GT Power software to predict the exhaust residual gas fraction with an advanced intake valve opening strategy. Their results showed that an increase in internal exhaust gas recirculation led to increased ignition delay and combustion duration, and decreased NO_x emissions. The effect of internal exhaust recirculation was more sensitive when the dual-fuel mode was applied.

Lei Zhou et al. [16] evaluated a single-cylinder, four-stroke Ricardo E6 to study the influence of exhaust gas recirculation on the engine combustion characteristics under low load conditions. The intake valve timing and exhaust valve timing were used to adjust the exhaust residual gas ratio. They found that under partial load conditions, when the exhaust residual gas ratio was small, the heating effect was the main influence on the burning rate, but when the exhaust residual gas ratio was larger, the burning rate was reduced. Under idle conditions, the combustion stability and fuel consumption were improved with a larger residual gas ratio. Jun Yang et al. [17,18] presented a statistical dynamic model with stochastic properties that was developed to control the exhaust residual gas in gasoline engines. In further research, they used that dynamic model to investigate the influence of the transient residual gas fraction on engine power. They found that the exhaust residual gas fraction has a sensible influence on misfiring, NO_x emission, the heat release rate, and engine knocking.

Mingzhang et al. [19] studied the effect of internal exhaust gas recirculation on the emission characteristics and ignition stability of a gasoline compression ignition engine. In their research, the internal exhaust gas ratio was increased from 10 to 90%, the engine operated at low load condition. From the results, they found that the ignition stability could be improved and optimal ignition delay time was obtained when internal exhaust gas rates from 30 to 60%. With an excess air ratio was 1.0 or 1.5 and internal exhaust gas rate from 20 to 60% a high engine torque could be presented. A suitable internal exhaust gas rate helps to decrease HC, CO and NO_x emission.

In summary, most previous studies did not present in detail the sensitive parameters that distribute exhaust residual mass trapped in the cylinder, such as intake and exhaust valve timing, engine speed, air-to-fuel ratio, combustion duration, engine load, and intake and exhaust pressure. That research only focused on adjusted intake and exhaust valve timing to control the exhaust residual, and this was specifically accomplished by modifying the engine's original valve mechanics system or manufacturing several camshafts. Those methods were limited because of material consumption, higher cost and longer production time and difficulties in maintaining the same testing environmental conditions in the experiments. Further, because those experiments were conducted in limited experimental conditions with changing valve timings, the validation of the simulation model was also limited. This may results in largely inaccurate of the simulation model in prediction of the exhaust residual gas. All of these drawbacks are significant gaps in the extant literature, and this gap will be filled up through the research of this paper.

Through experimental and simulation approach method, the effects of engine speed, air–fuel ratio, valve overlap, combustion duration, intake port diameter-bore ratio, and bore-stroke ratio on the internal exhaust residual gas recirculation and the effect of residual gas on the

effective release energy, peak firing pressure rise, and engine emission characteristics was investigated.

2. Methodology

2.1. Experiment setup

A small gasoline, spark ignition engine with 137 Cm^3 of a cylinder's displacement was carried out. The highest intake valve lift is 6.5 mm and highest exhaust valve lift is 6.4 mm. The inlet port diameter is 22 mm, and that of the exhaust valve port was 19 mm. The engine test speed was 5000 rpm and the ignition timing was 30 deg BTDC, and the air–fuel ratio is 13.6. The environmental temperature was maintained in 29.5–30 °C. Air flow was used for coolant, the temperature of lubricant oil was 80 °C, and the throttle was opened 90 degrees. The pressure of fuel was 333–362 kPa. The experiments were conducted on the steady state condition. The experimental equipment was calibrated before use. The applicable engine specifications are shown in Table 1.

The schematic of the experimental system is shown in Fig. 1 and Fig. 2 presents engine testing system. The system consisted of 22 parts: a dynamo controller (1), an AVL dynamometer (2), a connecting shaft (3). On the experimental engine (4) the flywheel (5), the encoder (E40S8-1800-3-T-24) (6) and the temperature sensor (7) was located. The fuel tank (8) supplies gasoline fuel to the injector (11) through the gasoline pump (9) and the gasoline fuel filter (10). Air flow was cleaned by the air cleaner box (15) and into the cylinder through throttle (16). An air heater (17) was employed to maintain the air flow temperature. The exhaust gas analyzer (Horiba MEXA-7100DEGR), cylinder pressure transducer (Kistler 6056A) (19), ECU (20), data acquisition device (21), and computer (22) received signals from the oxygen sensor (12), the exhaust gas temperature sensor (13), the cylinder pressure sensor (14), and the throttle angle and air mass from the sensor (18).

2.2. Simulation modeling

It is complicated to investigate the trapped residual gas ratio, the effective release energy, and to estimate the parameters which affected the internal exhaust residual gas recirculation under the various operating conditions. Simulation is effective and useful tools to solve the problem, so we used the well-known AVL-Boost v. 2018 software which is able to simulate the SI engines [20], CI engines [21,22], turbocharged diesel engines [23,24], and alternative fuels engines [25]. We estimated the residual gas, the peak firing pressure rise, the combustion duration, and the effective release energy, all of which had significant effects on the engine emissions and performance. Our simulation results also showed the influence of internal residual gas on the effective energy. The simulation model is presented in Fig. 3.

All the parts of the research engine were defined in the simulation model. The engine steady state operation condition is activated through element E1. The simulation output data could be observed on the element monitor MNT1. The SB_1, SB_2 depicts the boundaries of the pipe system, and the element CL_1 is as an air cleaner. The throttle angle is controlled through element TH_1. The restriction R_1, R_2, and R_3 are used to control the pressure losses on the pipe system (1–21). The air flow of the system is distributed or collected by the junctions J1-6, and the flow temperature, flow pressure, and mass flow is determined through element $MP_{1\text{-}2}$. Gasoline fuel is injected into the cylinders ($C_{1\text{-}2}$) via the two injectors $I_{1\text{-}2}$.

Combustion model:

The heat release characteristics of the engine model as follows the Vibe function:

$$\frac{dx}{d\alpha} = \frac{a}{\Delta\alpha}(m+1)y^m.e^{-a.y(m+1)} \quad (1)$$

$$dx = \frac{dQ}{Q}; y = \frac{\alpha-\alpha_0}{\Delta\alpha_c}$$

The mass fraction burned χ is calculated:

$$x = \int \frac{dx}{d\alpha}d\alpha = 1 - e^{-a.y(m+1)} \quad (2)$$

The heat transfer of the combustion chamber is following Woschni's model:

$$Q_T = A.q_{coeff}.(T_c - T_w) \quad (3)$$

where:

The flow rate of the air mass through the exhaust and intake ports were estimated via Eqs. (4) and (5):

$$\frac{dm}{dt} = A_{eff}P_1\sqrt{\frac{2}{RT_1}}.C \quad (4)$$

$$C = \sqrt{\frac{K}{K-1}[(\frac{P_2}{P_1})^{\frac{2}{k}} - (\frac{P_2}{P_1})^{\frac{K+1}{K}}]} \quad (5)$$

The residual gas was calculated from Eq. (6):

$$x_{SOC}^{cp} = \frac{\int_{V_c}^{V}\rho.x^{cp}.dV}{\int_{V_c}^{V}\rho.dV} \quad (6)$$

The NO_x formation is determined from the reactions [26,27] in Table 2:

The concentration of N_2O and NO rate is calculated from Eqs. (7) and (8):

$$C_{N_2O} = 1.1802.10^{-6}.T^{0.6125}.e^{\frac{94716}{T}}.C_{N_2}.\sqrt{P_{O_2}} \quad (7)$$

$$r_{NO} = 2.C_{p.}.C_K.[1-\lambda^2]\frac{r_1}{1+\lambda.R_1}.\frac{r_4}{1+R_2} \quad (8)$$

$$\lambda = \frac{C_{NO,act}}{C_{NO,equ}}.\frac{1}{C_P}; R_1 = \frac{r_1}{r_2+r_3}; R_2 = \frac{r_4}{r_5+r_6}$$

The CO formation is determined from the reactions [26,28] in Table 3:

The CO production is determined by the Eq. (9):

$$r_{CO} = C_{Const}.(r_1+r_2)(1-\theta) \quad (9)$$

$$\theta = \frac{C_{NO,act}}{C_{NO,equ}}$$

The mass of unburned HC was calculated by Eq. (10) [26,29]:

$$m_{HC} = \frac{P_C.V_{crevice}.M}{R.T_{piston}} \quad (10)$$

The essential input and output data of simulation model is shown in table 4:

Table 1
Engine specifications.

Parameter	Unit	Value
Engine model	–	Four stroke, Spark ignition
Number of cylinder	–	2(V-Twin)
Compression ratio	–	11.8:1
Bore	mm	57
Stroke	mm	53.8
Connecting rod	mm	107.9
Intake valve	–	2
Exhaust valve	–	2
Cooling system	–	Air cooled

3. Results and discussions

The engine parameters affected in internal exhaust residual gases

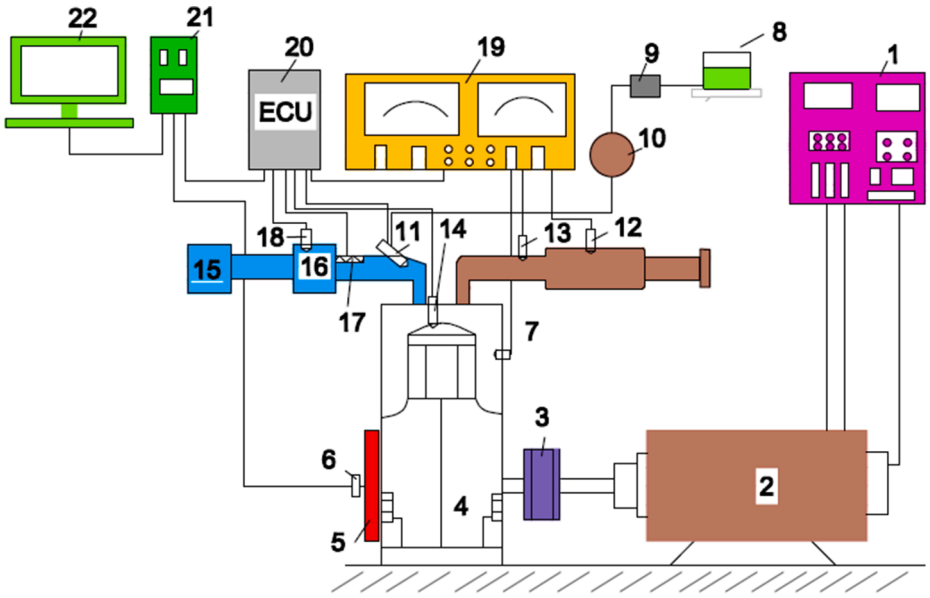

Fig. 1. Schematic of experimental engine system.

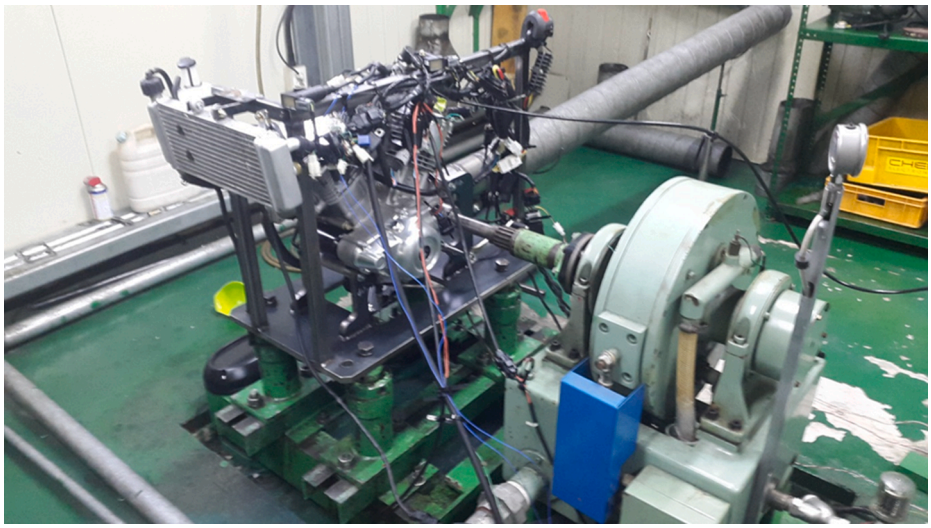

Fig. 2. The experimental engine system.

recirculation and the influence of internal exhaust residual gas on the effective energy and emission formation of a spark ignition at normal engine operation 5000 rpm will be completely discussed in below.

3.1. Model validation

The experiments were conducted to supply basic engine performance data which were used to validate the simulation model. Figs. 4–9 shows the comparison between the experimental and simulation output data. The black line describes the experiment results while the red lines describe the simulated results. Since the ignition timing was input data of simulation model so a similar ignition timing value of two cases is presented in Fig. 4.

From the simulated model, the air mass flow was adjusted via the engine flow coefficient (exhaust ports and intake pipes). Fig. 5 shows the maximum difference of air mass flow is 3.1% at 6000 rpm. The air mass is an average of the experimental values and is thus acceptable. When the air–fuel ratio was constant, the fuel was supplied into the cylinder was depended on the air mass flow; this mass of injected fuel influences the combustion temperature and combustion pressure rise. Figs. 6 and 7 show the validated peak firing temperature and peak pressure rise. The same trends can be observed in the experimental and simulation data values. The maximum differences in the peak firing temperature and peak pressure rise were 5.34% and 4.5%, respectively.

Fig. 8 compares the simulation brake torque and experiment brake torque. The engine archives the maximum brake torque of 21.8 Nm at 7000 rpm, the maximum difference of 2.47% was notified at 8000 rpm. Fig. 9 compares the engine NO_x emission. Because NO_x emission is an important indicator of toxic engine emission characteristics, it was selected as an important factor in validating the simulation emission characteristics. With increased engine speed, the NO_x emission increased until a maximum value was achieved, after which the emission decreased. We observed that the engine NO_x emission was fairly well correlated with different engine speeds; the maximum difference was 6.58%.

After the validation, a steady simulation model provides an accurate method to predict the engine performance and emission formation. The influence of engine parameters on internal exhaust gas recirculation and

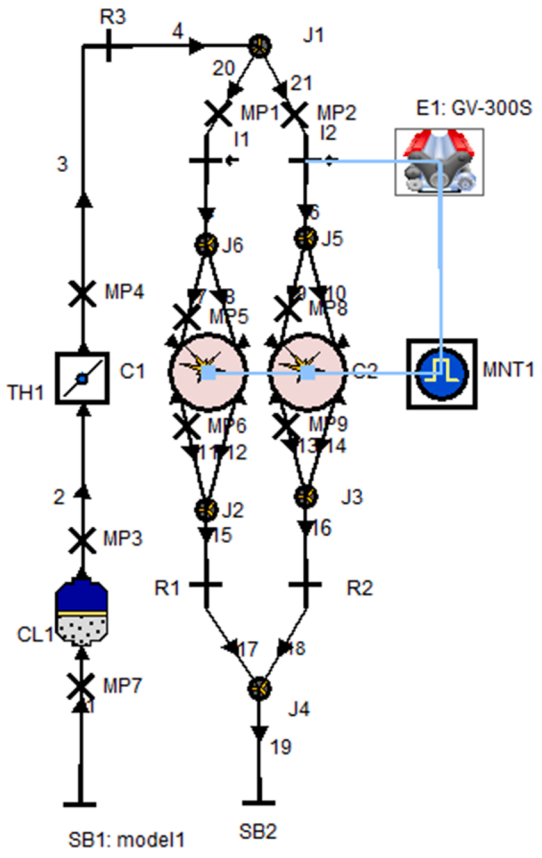

Fig. 3. Simulation model.

Table 2
NO_x formative reactions.

Stoichiometry	Rate $k_i = k_{0,i}.\ T^a.\ e^{(-TA_i/T)}$	k_0 [cm^3, mol, s]	a [–]	T_A [K]
$N_2 + O = NO + N$	$r_1 = k_1\ .\ C_{N2}.\ C_O$	4.93E13	0.0472	38048.01
$O_2 + N = NO + O$	$r_2 = k_2\ .\ C_{O2}.\ C_N$	1.48E08	1.5	2859.01
$N + OH = NO + H$	$r_3 = k_3\ .\ C_{OH}.\ C_N$	4.22E13	0.0	0.0
$N_2O + O = NO + NO$	$r_4 = k_4\ .\ C_{N2O}.\ C_O$	4.58E13	0.0	12130.6
$O_2 + N_2 = N_2O + O$	$r_5 = k_5\ .\ C_{O2}.\ C_{N2}$	2.25E10	0.825	50569.7
$OH + N_2 = N_2O + H$	$r_6 = k_2\ .\ C_{OH}.\ C_{N2}$	9.14E07	1.148	36190.66

Table 3
CO formative reactions.

Stoichiometry	Rate
$CO + OH = CO_2 + H$	$r_1 = 6{,}76\ .\ 10^{10}.\ e^{(T/1102)}.C_{CO}.C_{OH}$
$CO + O_2 = CO_2 + O$	$r_2 = 2{,}51\ .\ 10^{12}.\ e^{(-24055/T)}.C_{CO}.C_{O2}$

the effect of exhaust residual fraction on engine performance and emission could be estimated via this simulation model.

3.2. Estimation of parameters affected in internal exhaust residual gases recirculation

We here thoroughly discuss and summarize the parameters affected in internal exhaust residual gases recirculation of an engine, which has not been presented elsewhere in the literature. Fig. 10 presents the residual gas ratio versus engine speed. The engine speed has a sensitive effect on the residual gas ratio; in our study, when the engine speed increased from 3000 to 10,000 rpm, the residual gas ratio decreased

Table 4
The essential input and output data of the simulation model.

Input data	Unit	Output data	Unit
Intake pipes length and diameter	mm	Engine brake torque	Nm
Exhaust pipes length and diameter	mm	Engine power	kW
Throttle diameter	mm	IMEP, BMEP, FMEP	bar
Throttle angle	deg	ISFC, BSFC	g/kWh
Bore, Stroke, connecting rod length	mm	Peak temperature	K
Intake and exhaust valve lift versus crankshaft angle	mm	Peak pressure rise	Bar/deg
Intake and exhaust port diameter	mm	Peak pressure	bar
Engine friction	bar	Internal and external residual gas	–
Compression ratio	–	Volumetric efficiency	–
Air-fuel ratio	–	Heat losses (piston, cylinder head, cylinder liner)	kJ
Air flow coefficient on the pipes, ports	–	Effective release energy	kJ
Ignition timing	deg	Exhaust gas temperature	K
Piston, cylinder head and liner surface area	mm^2	Exhaust gas pressure	bar
Ambient temperature and pressure	deg C and bar	NO_x emission	g/kWh
Air cleaner volume	liter	HC emission	g/kWh
Fuel type	–	CO emission	g/kWh

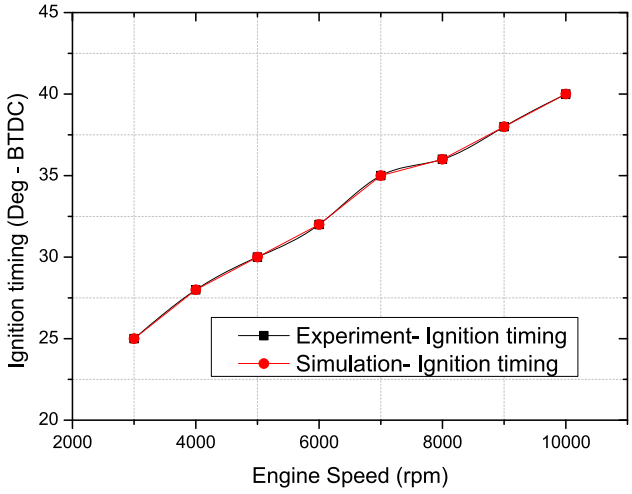

Fig. 4. Ignition timing validation.

from 4.52% to 1.23%. This can be explained by the fact that the increase of engine speed led to increases in the velocity and inertia of the exhaust and intake gas flows. In the exhaust stroke, the increased velocity and inertia of the exhaust gas flow expelled more exhaust gas from inside the cylinder to the outside. During the intake stroke, the increased velocity and inertia of the intake airflow introduced fresher air–fuel mixture to sweep burned gas out from the combustion chamber.

Fig. 11 presents the residual gas ratio versus the air–fuel ratio (A/F ratio). The A/F ratio has an effective effect on the residual gas ratio; the exhaust residual gas ratio reduced from 3.18% to 2.58% when the A/F ratio increased from 12.5 to 15. This can be explained by the fact that the increase in the A/F ratio introduced fresh air mass into the cylinder while the fuel mass was kept constant. The increase in fresh air mass in the cylinder not only swept the exhaust residual gas out of the cylinder, but also helped to reduce the molecularly multiform exhaust gases.

There are three positive valve overlap configurations (Fig. 12):

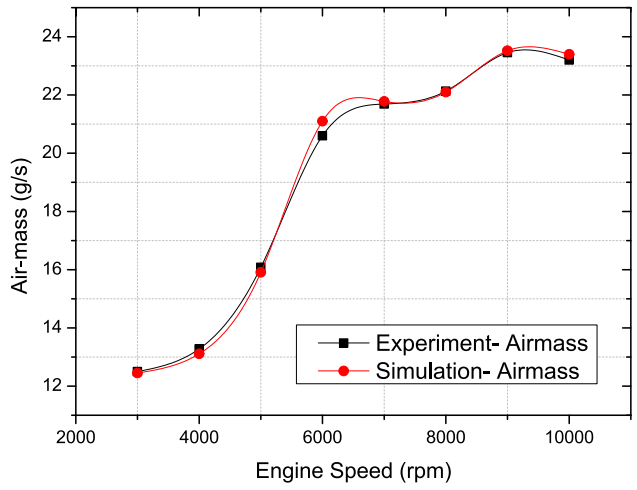

Fig. 5. Air mass flow validation.

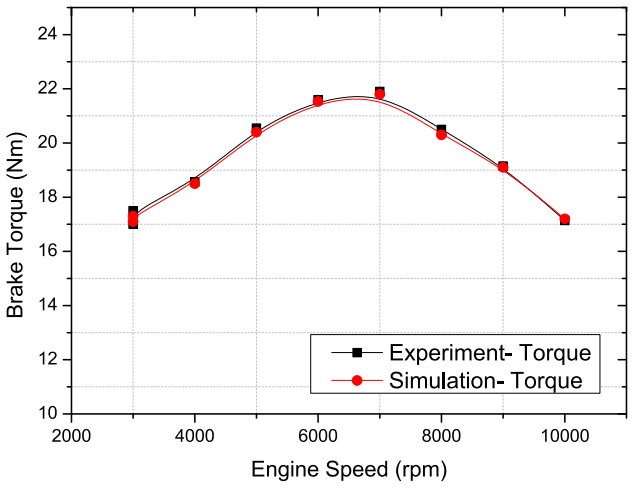

Fig. 8. Brake torque validation.

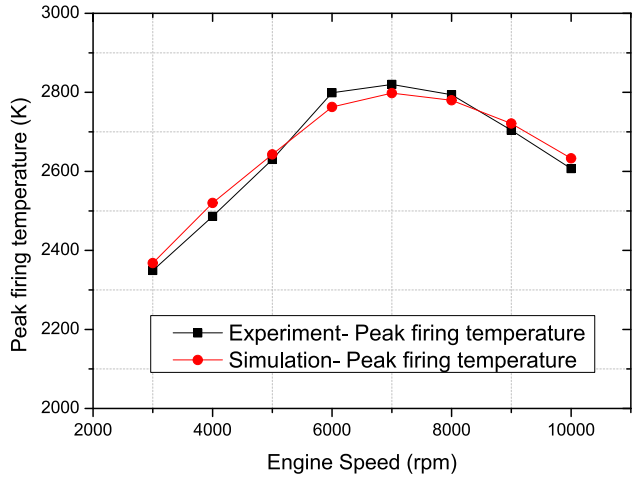

Fig. 6. Peak firing temperature validation.

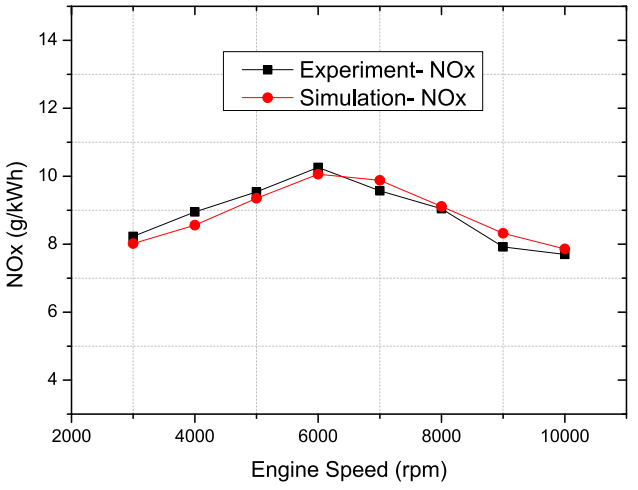

Fig. 9. NO_x emission validation.

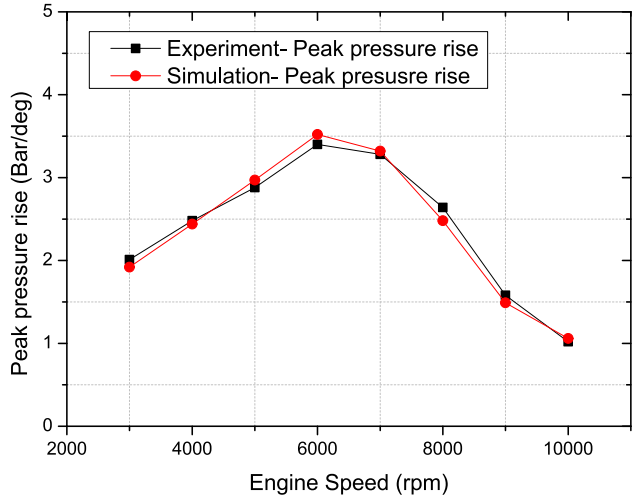

Fig. 7. Peak firing pressure rise validation.

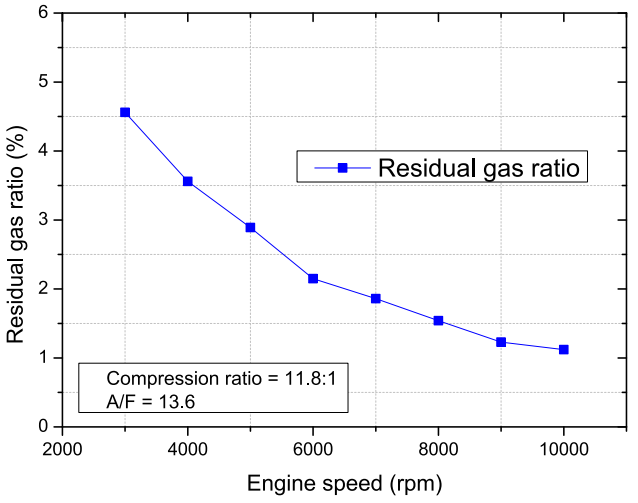

Fig. 10. Exhaust residual gas ratio versus engine speed.

intake valve early opening (IVEO); exhaust valve late closing (EVLC), and combined IVEO&EVLC.

Here, the effect of each valve timing configuration on the residual gas ratio is presented. As shown in Fig. 13, when the valve overlap increased, all three configurations showed an uptrend in the residual gas ratio. In a combustion engine the intake valve timing is known to affect the inlet air flow into the cylinder; conversely, the exhaust valve timing

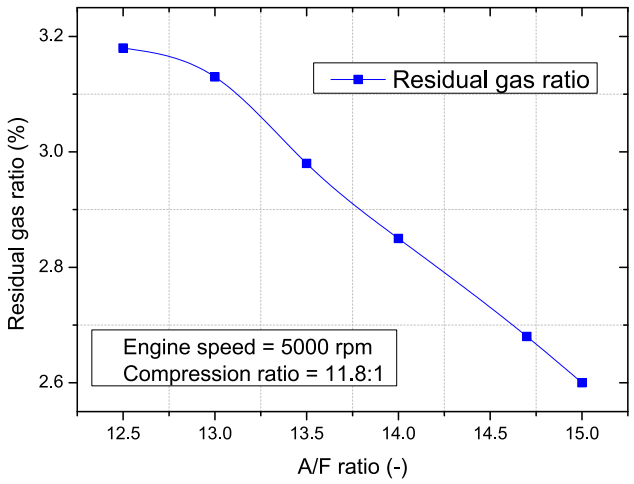

Fig. 11. Exhaust residual gas ratio versus A/F ratio.

strongly affects the exhaust gas flow. A higher fresh air–fuel mixture will be charged and more burned gas will be discharged from combustion chamber with a suitable valve overlap. But an early valve overlap causes the exhaust gas is expelled into the inlet port, and a late valve overlap may result in the reverse flow, which would return the exhaust gas back into the combustion chamber. This explains why the IVEO&EVLC configuration of valve overlap has a greater effect on the residual gas ratio than the other configurations.

In our previous publication [30] we discussed the effect of combustion duration on engine operation and emission formation of a V-twin engine at 6000 rpm, 7000 rpm, and 8000 rpm. In this paper, to avoid duplicating the data were taken at 5000 rpm (Fig. 14). Longer combustion duration leads to increase the residual gas ratio because the burning process may extend until the pistons are at bottom dead center (BDC) or even in the exhaust stroke. This process increases the reverse flow which would return the exhaust residual gas into the cylinder. This explains why the exhaust residual gas ratio increased from 0.9% to 1.53% when combustion duration rose from 30 to 100 deg CA.

Fig. 15 shows the effect of intake port diameter-bore ratio (IPD/B ratio) on the residual gas. Here the IPD/B ratio rose from 0.3 to 0.5; the intake valve port diameter at 22 mm is the reference value. With each change of the intake valve port diameter value, the bore diameter was kept constant at 57 mm. When the IPD/B ratio increased from 0.3 to 0.5, the residual gas ratio decreased from 2.96% to 2.7% the increased IPD/B ratio at high engine speed led to decreased airflow restriction of the inlet port. The subsequent effect of the intake stroke was to increase the amount of fresh air fill into the cylinder, which swept the exhaust residual gas to outside. This is why the residual gas ratio decreased as the IPD/B ratio increased.

Fig. 16 presents the effect of bore-stroke ratios on the residual gas. The band of bore-stroke ratio was from 0.8 to 1.1 and the reference value is 1.06. The length of connecting rod was modified to maintain constant compression ratio. In the band of bore-stroke, the residual gas ratio fluctuated within 5%. The smallest of residual gas ratio was 2.8% at a 0.8 bore-stroke ratio, and the biggest residual gas ratio was 2.85% at a 0.88 bore-stroke ratio. This could be explained by that a bigger bore-stroke ratio promoting raised air–fuel mass and longer combustion duration. The increased air–fuel mass was due to the decreased residual gas ratio, but the increased combustion duration was due to the higher exhaust residual gas ratio.

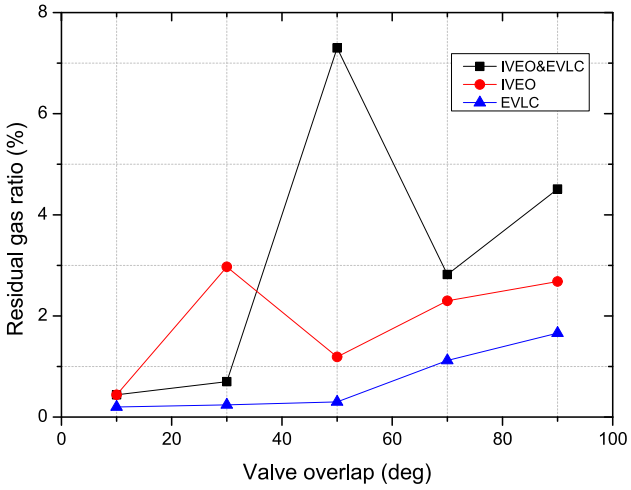

Fig. 13. Exhaust residual gas ratio versus valve overlap.

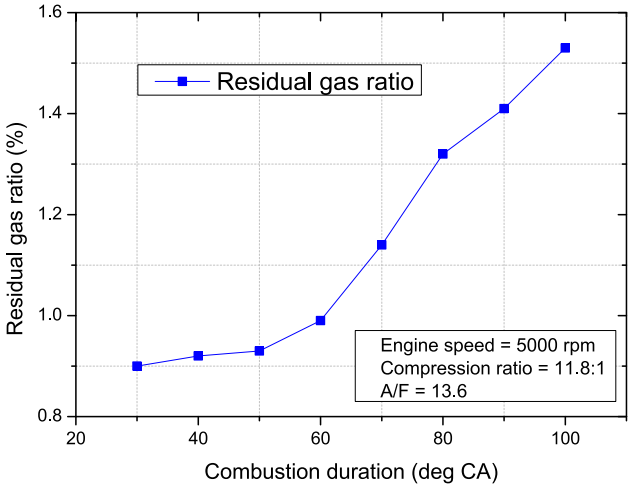

Fig. 14. Exhaust residual gas ratio versus combustion duration.

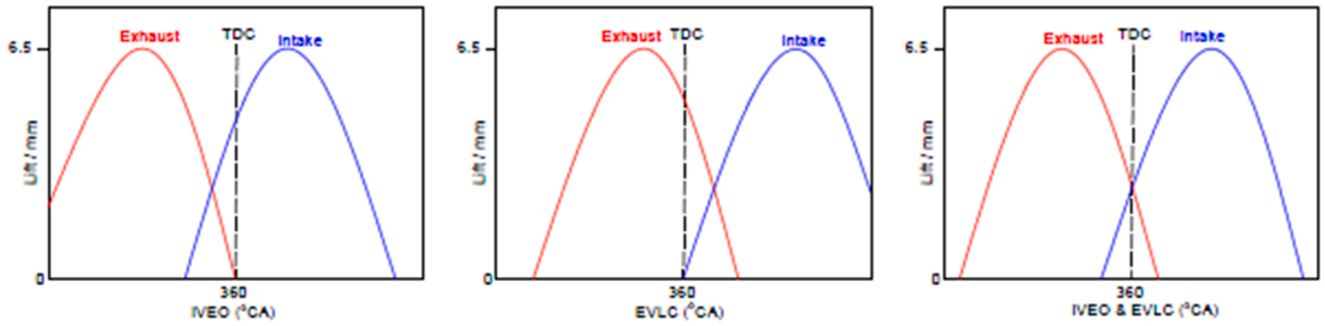

Fig. 12. Positive valve overlap configurations.

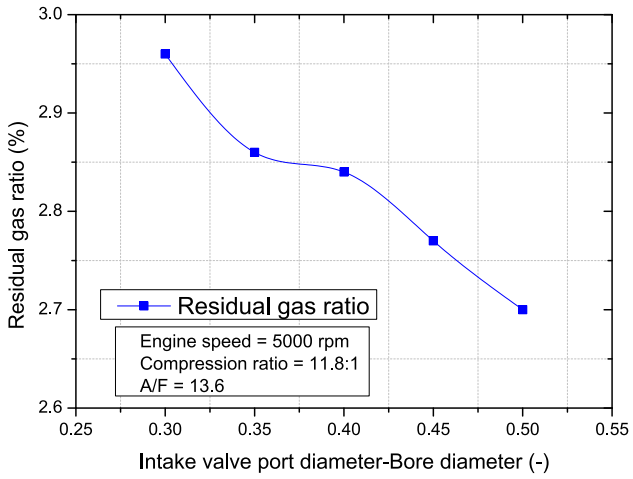

Fig. 15. Exhaust residual gas ratio versus IPD/B ratio.

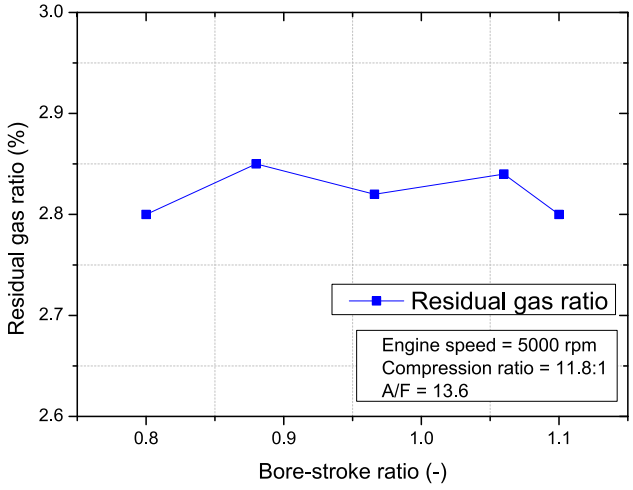

Fig. 16. Exhaust residual gas ratio versus Bore-Stroke ratio.

3.3. The effect of residual gas on peak pressure rise, effective release energy and engine emission characteristics

The exhaust residual gas ratio has a sensitive effect on peak temperature and peak pressure rise. As shown in Figs. 17 and 18, the peak temperature and peak firing pressure rise decreased when the exhaust residual gas increased. This is because the increase in exhaust residual gas in the cylinder was due to a diluted and less homogeneous air–fuel mixture and an increased area that lacked fuel or oxygen. As a result, when the exhaust residual gas rose from 1% to 5%, the peak firing temperature decreased from 2900 K to 1250 K and the peak pressure rise decreased from 8 to 5.5 bar/deg.

In the power stroke, the chemical energy of fuel trapped in the cylinder is released into heat energy. A certain amount heat energy is lost from heat transfer and other amount energy is not released (but instead goes into the combustion products), and the remaining heat energy is the effective release energy. The heat transfer loss and combustion duration have a sensitive effect on the effective release energy. Fig. 19 shows a decline in effective release energy as the exhaust residual gas increased. This could have been because the combustion reaction does not occur instantaneously in a typical SI engine so the heat isn't instantaneously released at the top dead center (TDC) [24]. To improve the engine thermal efficiency, a short burn time leads to the faster release of the heat energy. When this is the case, the increased heat energy released in an actual cycle and a typical Otto cycle would be similar. Conversely, the

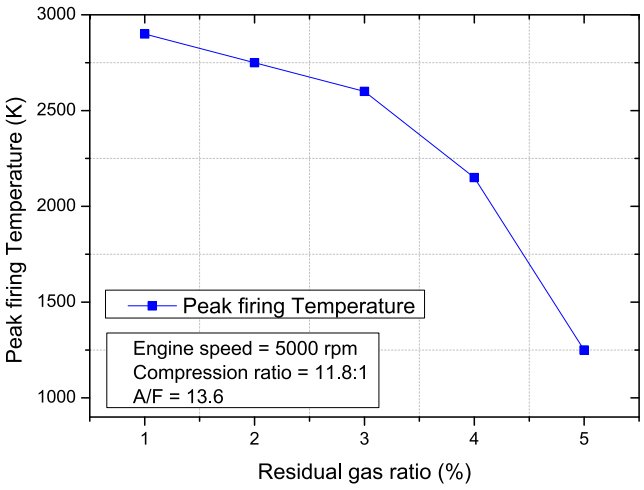

Fig. 17. Peak firing temperature versus residual gas ratio.

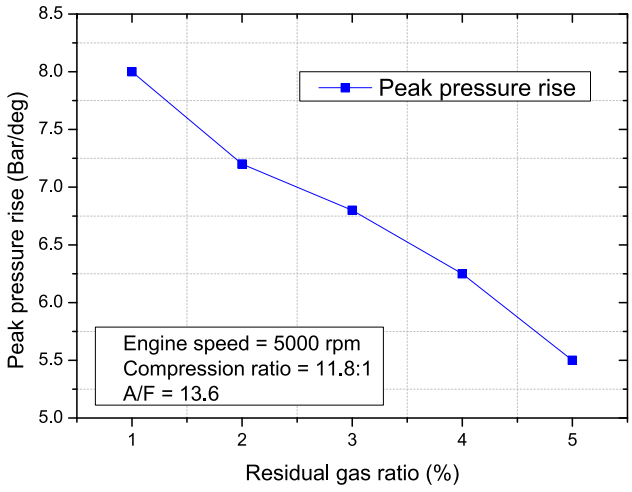

Fig. 18. Peak firing pressure rise versus residual gas ratio.

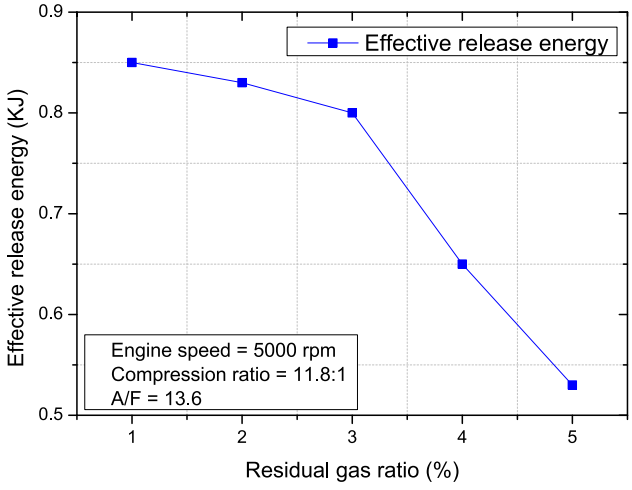

Fig. 19. Effective release energy versus residual gas ratio.

increase of residual gas in the cylinder due to a longer burn time, lower peak firing pressure rise, and lower peak firing temperature leads to a lower effective release energy. In this study, the effective release energy decreased from 0.85 KJ to 0.53 KJ when the residual gas ratio increased

from 1% to 5%.

Figs. 20 and 21 show the influence of exhaust residual gas on IMEP and BMEP. The BMEP and IMEP were decreased when the residual gas ratio increased because the latter had the similar influence on BMEP, IMEP, and the effective release energy. Figs. 19, 20, and 21 present same trends of effective release energy, IMEP and BMEP. Equation (11) shows the relationship between BMEP and IMEP, explaining why the engine achieved BMEP and IMEP at the same value of the residual gas ratio:

$$BMEP = IMEP - FMEP - SMEP \tag{11}$$

When the residual gas ratio was 1%, the maximum BMEP was 9.48 bar and maximum IMEP was 11.6 bar. At the residual gas ratio of 5%, the minimum values of BMEP and IMEP were 4.3 bar and 6.5 bar, respectively.

Fig. 22 shows the influence of exhaust residual gas on BSFC, trending downward when the residual gas ratio increased from 1% to 5%. In testing conditions with constant engine speed and a constant air–fuel ratio, the BMEP had the greatest effects on the BSFC. The relationship between BMEP and BSFC is described in Eq. (12):

$$BSFC = \frac{m_{air}.n_c.2.16.10^9}{AFR.BMEP.V_D.n} \tag{12}$$

The contrary trends of BMEP and BSFC are depicted in Figs. 21 and 22, respectively. The engine achieved its minimum BSFC (350 g/kWh) when the BMEP was at the maximum value, and the maximum BSFC was 720 g/kWh when the BMEP was at the minimum value.

Eq. (13) shows that a decrease of BMEP led to a reduction engine effective torque.

$$T_{eff} = \frac{BMEP.V_D}{k_{cycle}.\pi} \tag{13}$$

Fig. 23 presents the influence of the residual gas ratio on the engine torque. With an increasing residual gas ratio, the BMEP and engine brake torque showed the same downward trends. At a residual gas ratio of 1%, the engine's maximum brake torque was 20.3 Nm.

Fig. 24 shows the NO_x emission versus residual gas ratio. The NO_x emissions tend to decrease with an increasing residual gas ratio for two reasons. First, an increased residual ratio is associated with a decreased peak firing temperature. And second, an increase in the residual gas is caused by a diluted air–fuel mixture and a lower level of oxygen concentrate. The decreased oxygen concentrate leads to decreased NO_x emissions in the combustion stroke. In our study, these two factors explain why the NO_x tended to decrease with an increasing residual gas ratio. The minimum NO_x emission was 2.12 g/kWh at a 5% residual gas ratio.

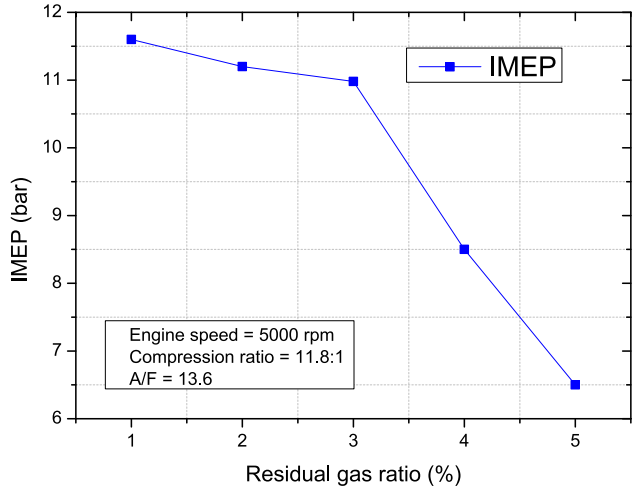

Fig. 20. IMEP versus residual gas ratio.

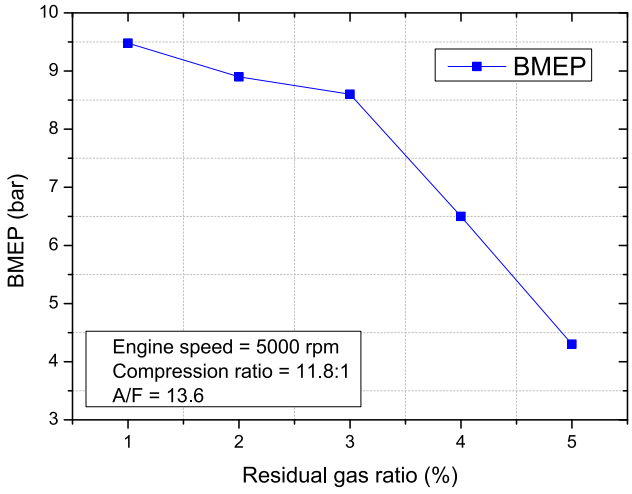

Fig. 21. BMEP versus residual gas ratio.

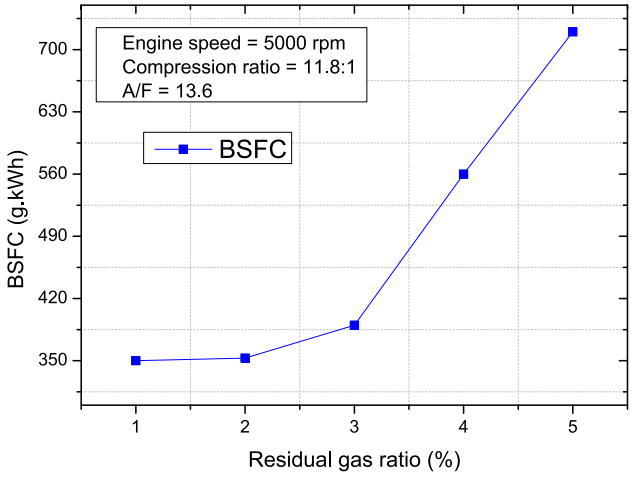

Fig. 22. BSFC versus residual gas ratio.

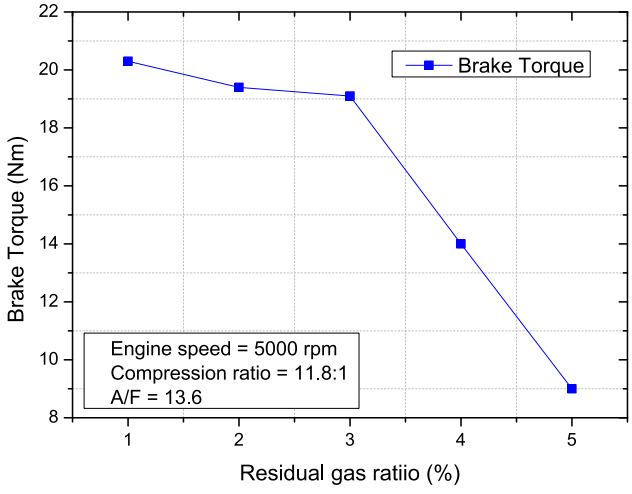

Fig. 23. Brake torque versus residual gas ratio.

Figs. 25 and 26 show the CO and HC emissions versus residual gas ratio. An increased residual gas ratio leads to a diluted air–fuel mixture and increased areas lacking oxygen. In this study, the dilution of the air–fuel mixture and the lack of oxygen increased the unburned HC and

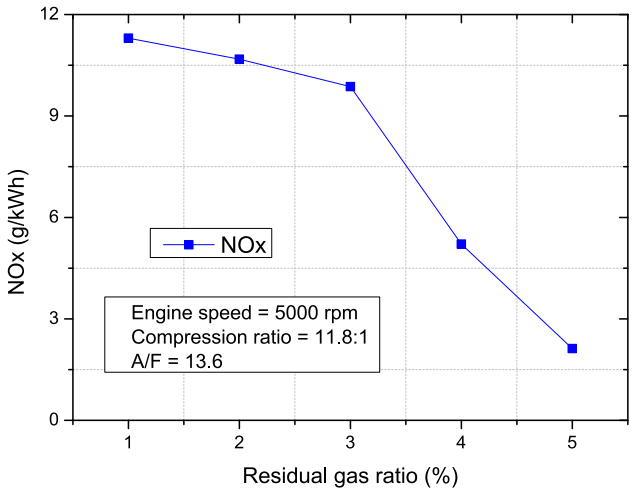

Fig. 24. NO_x emission versus residual gas ratio.

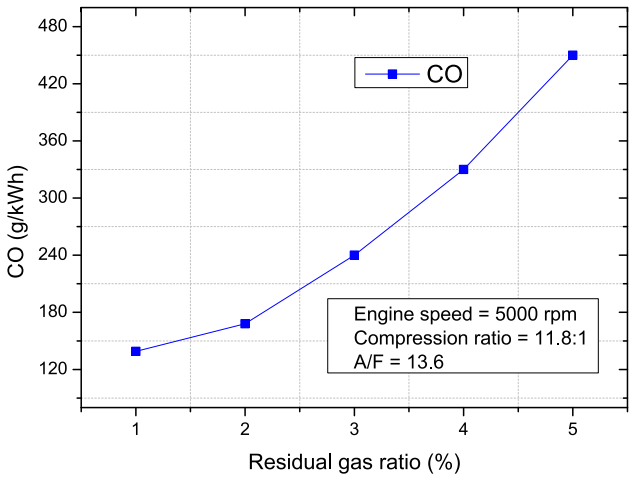

Fig. 25. CO emissions versus residual gas ratio.

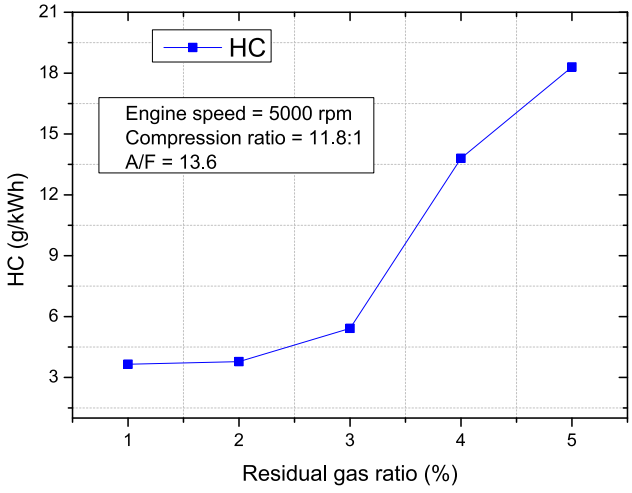

Fig. 26. HC emissions versus residual gas ratio.

CO emissions from 3.65 to 18.2 g/kwh and from 139 to 450 g/kwh, respectively.

4. Conclusions

In this study, using an experimental and simulation approach, we eliminated certain drawbacks of earlier experimental optimization methods. We thoroughly investigated the parameters which have sensitive effects on internal exhaust residual gas recirculation, as well as the influence of exhaust residual gas on the effective release energy and engine emission characteristics of an SI V-twin engine. We here report on our new, accurate method to determine the residual gas, effective release energy, and engine emission characteristics.

We found:

(1) The residual gas ratio decreased from 4.52% to 1.23% when the engine speed increased from 3000 to 10,000 rpm. The A/F ratio and valve overlap had sensitive effects on the residual gas ratio, which decreased from 3.18% to 2.58% when the A/F ratio increased from 12.5 to 15. Also, an optimal valve overlap allowed a fresh air–fuel mixture into the cylinder and carried more exhaust gas out of the combustion chamber. The IVEO&EVLC case of valve overlap had a greater effect on the residual gas ratio than that at the IVEO case and the EVLC case.

(2) When the IPD/B ratio increased from 0.3 to 0.5, the residual gas ratio decreased from 2.96% to 2.7%. But when the bore-stroke ratio increased from 0.8 to 1.1, the residual gas ratio was fluctuated within 5%. The minimum residual gas ratio was 2.8% at a 0.8 bore-stroke ratio, and the maximum residual gas ratio was 2.85% at a 0.88 bore-stroke ratio.

(3) When the residual gas ratio increased from 1% to 5%, the peak firing temperature decreased from 2900 to 1250 K and the peak pressure rise decreased from 8 to 5.5 bar/deg. The effective release energy decreased from 0.85 KJ to 0.53 KJ. The IMEP decreased from 11.6 to 6.5 bar, the BMEP decreased from 9.48 to 4.3 bar, and the engine brake torque decreased from 20.3 to 9 Nm. The NO_x emission declined from 11.3 to 2.12 g/kwh and the HC and CO emissions increased from 3.65 to 18.2 g/kwh and from 139 to 450 g/kwh, respectively.

CRediT authorship contribution statement

Nguyen Xuan Khoa: Conceptualization, Methodology, Writing - review & editing. **Y. Quach Nhu:** Formal analysis, Resources. **Ocktaeck Lim:** Supervision, Project administration.

Declaration of Competing Interest

The authors declare that they have no known competing financial interests or personal relationships that could have appeared to influence the work reported in this paper.

Acknowledgement

This work was supported by the 2020 Research Fund of University of Ulsan, South Korea.

References

[1] Venu H, Subramani L, Raju VD. Emission reduction in a DI diesel engine using exhaust gas recirculation (EGR) of palm biodiesel blended with TiO2 nano additives. Renew Energy 2019;140:245–63. https://doi.org/10.1016/j.renene.2019.03.078.

[2] Verschaeren R, Schaepdryver W, Serruys T, Bastiaen M, Vervaeke L, Verhelst S. Experimental study of NOx reduction on a medium speed heavy duty diesel engine by the application of EGR (exhaust gas recirculation) and Miller timing. Energy 2014;76(x):614–21. https://doi.org/10.1016/j.energy.2014.08.059.

[3] Wang D, Shi L, Zhu S, Liu B, Qian Y, Deng K. Numerical and thermodynamic study on effects of high and low pressure exhaust gas recirculation on turbocharged marine low-speed engine. Appl Energy 2019;261(April 2020):114346. https://doi.org/10.1016/j.apenergy.2019.114346.

[4] Pan M, et al. Reduction in PM and NOX of a diesel engine integrated with n-octanol fuel addition and exhaust gas recirculation. Energy 2019;187(X):115946. https://doi.org/10.1016/j.energy.2019.115946.

[5] Lattimore T, Wang C, Xu H, Wyszynski ML, Shuai S. Investigation of EGR Effect on Combustion and PM Emissions in a DISI Engine. Appl Energy 2016;161(x):256–67. https://doi.org/10.1016/j.apenergy.2015.09.080.
[6] Jung D, Lee S. An investigation on the potential of dedicated exhaust gas recirculation for improving thermal efficiency of stoichiometric and lean spark ignition engine operation. Appl Energy 2018;228(July):1754–66. https://doi.org/10.1016/j.apenergy.2018.07.066.
[7] Jiang C, Huang G, Liu G, Qian Y, Lu X. Optimizing gasoline compression ignition engine performance and emissions: Combined effects of exhaust gas recirculation and fuel octane number. Appl Therm Eng 2019;153(January):669–77. https://doi.org/10.1016/j.applthermaleng.2019.03.054.
[8] Cairns A, Zhao H, Todd A, Aleiferis P. A study of mechanical variable valve operation with gasoline-alcohol fuels in a spark ignition engine. Fuel 2013;106:802–13. https://doi.org/10.1016/j.fuel.2012.10.041.
[9] Fontana G, Galloni E. Variable valve timing for fuel economy improvement in a small spark-ignition engine. Appl Energy 2009;86(1):96–105. https://doi.org/10.1016/j.apenergy.2008.04.009.
[10] Khoa NX, Lim OT. Effective release energy, residual gas, and engine emission characteristics of a V-twin engine with various exhaust valve closing timings. J. Mech. Sci. Technol. 2020;34(1). https://doi.org/10.1007/s12206-019-1245-6.
[11] Velmurugan V, Aathif Akmal SM, Paramasivam V, Thanikaikarasan S. Prediction of vibration and exhaust gas emission characteristics using palm oil with nano particle diesel fuel. Mater Today Proc 2020;21(xxxx):800–5. https://doi.org/10.1016/j.matpr.2019.07.248.
[12] Binnig S, Fuchs S, Robles Collantes CA, Volpp HR. Exhaust gas condensate – formation, characterization and influence on platinum measuring electrodes in diesel vehicles. Sensors Actuators, B Chem 2017;242(x):1251–8. https://doi.org/10.1016/j.snb.2016.09.082.
[13] Lanzanova TDM, Dalla Nora M, Martins MES, Machado PRM, Pedrozo VB, Zhao H. The effects of residual gas trapping on part load performance and emissions of a spark ignition direct injection engine fuelled with wet ethanol. Appl. Energy 2019;253(x):113508. https://doi.org/10.1016/j.apenergy.2019.113508.
[14] Szwaja S, et al. Influence of exhaust residuals on combustion phases, exhaust toxic emission and fuel consumption from a natural gas fueled spark-ignition engine. Energy Convers Manag 2017;165(December 2018):440–6. https://doi.org/10.1016/j.enconman.2018.03.075.
[15] da Costa RBR, et al. Combustion, performance and emission analysis of a natural gas-hydrous ethanol dual-fuel spark ignition engine with internal exhaust gas recirculation. Energy Convers Manag 2019;195(May):1187–98. https://doi.org/10.1016/j.enconman.2019.05.094.
[16] Wei H, Shao A, Hua J, Zhou L, Feng D. Effects of applying a Miller cycle with split injection on engine performance and knock resistance in a downsized gasoline engine. Fuel 2017;214(June 2018):98–107. https://doi.org/10.1016/j.fuel.2017.11.006.
[17] Yang J, Sata K, Kako J, Ohata A, Shen T. Statistical model and control of residual gas mass in gasoline engines. IFAC 2013;7(PART 1).
[18] Sata K, Kako J, Yang J, Ohata A, Shen T. Effect of Transient Residual Gas Fraction for Gasoline Engines. IFAC 2013;46(21).
[19] Pan M, Qian W, Wei H, Feng D, Pan J. Effects on performance and emissions of gasoline compression ignition engine over a wide range of internal exhaust gas recirculation rates under lean conditions. Fuel 2019;265(November 2020):116881. https://doi.org/10.1016/j.fuel.2019.116881.
[20] Khoa NX, Lim O. Comparative Study of the Effective Release Energy, Residual Gas Fraction, and Emission Characteristics with Various Valve Port Diameter-Bore Ratios (VPD/B) of a Four-Stroke Spark Ignition Engine. Energies 2020;13(6):1330. https://doi.org/10.3390/en13061330.
[21] Pagán Rubio JA, Vera-García F, Hernandez Grau J, Muñoz Cámara J, Albaladejo Hernandez D. Marine diesel engine failure simulator based on thermodynamic model. Appl Therm Eng 2018;144(March):982–95. https://doi.org/10.1016/j.applthermaleng.2018.08.096.
[22] Petranović Z, Sjerić M, Taritaš I, Vujanović M, Kozarac D. Study of advanced engine operating strategies on a turbocharged diesel engine by using coupled numerical approaches. Energy Convers Manag 2018;171(May):1–11. https://doi.org/10.1016/j.enconman.2018.05.085.
[23] Teo AE, Chiong MS, Yang M, Romagnoli A, Martinez-Botas RF, Rajoo S. Performance evaluation of low-pressure turbine, turbo-compounding and air-Brayton cycle as engine waste heat recovery method. Energy 2019;166:895–907. https://doi.org/10.1016/j.energy.2018.10.035.
[24] Melaika M, Rimkus A, Vipartas T. Air Restrictor and Turbocharger Influence for the Formula Student Engine Performance. Procedia Eng 2017;187:402–7. https://doi.org/10.1016/j.proeng.2017.04.392.
[25] Praptijanto A, Muharam A, Nur A, Putrasari Y. Effect of ethanol percentage for diesel engine performance using virtual engine simulation tool. Energy Procedia 2015;68:345–54. https://doi.org/10.1016/j.egypro.2015.03.265.
[26] AVL. Theory AVL BOOST; 2011.
[27] Pattas K, Häfner G. Stickoxidbildung bei der ottomotorischen Verbrennung. MTZ 1973;12:397–404.
[28] Onorati A, Ferrari G, D'Errico G. 1D Unsteady Flows with Chemical Reactions in the Exhaust Duct-System of S.I. Engines: Predictions and Experiments. SAE 2001;01(0939).
[29] Derrico G, Ferrari G, Onorati A, Cerri T. Modeling the Pollutant Emissions from a S.I. EngineNo Title. SAE 2002;01:0006.
[30] Khoa NX, Lim O. The effects of combustion duration on residual gas, effective release energy, engine power and engine emissions characteristics of the motorcycle engine. Appl Energy 2019;248. https://doi.org/10.1016/j.apenergy.2019.04.075.